

# YOWOv2: A Stronger yet Efficient Multi-level Detection Framework for Real-time Spatio-temporal Action Detection

Jianhua Yang<sup>1</sup>, Kun Dai<sup>1</sup>

**Abstract**—Designing a real-time framework for the spatio-temporal action detection task is still a challenge. In this paper, we propose a novel real-time action detection framework, YOWOv2. In this new framework, YOWOv2 takes advantage of both the 3D backbone and 2D backbone for accurate action detection. A multi-level detection pipeline is designed to detect action instances of different scales. To achieve this goal, we carefully build a simple and efficient 2D backbone with a feature pyramid network to extract different levels of classification features and regression features. For the 3D backbone, we adopt the existing efficient 3D CNN to save development time. By combining 3D backbones and 2D backbones of different sizes, we design a YOWOv2 family including YOWOv2-Tiny, YOWOv2-Medium, and YOWOv2-Large. We also introduce the popular dynamic label assignment strategy and anchor-free mechanism to make the YOWOv2 consistent with the advanced model architecture design. With our improvement, YOWOv2 is significantly superior to YOWO, and can still keep real-time detection. Without any bells and whistles, YOWOv2 achieves 87.0% frame mAP and 52.8% video mAP with over 20 FPS on the UCF101-24. On the AVA, YOWOv2 achieves 21.7% frame mAP with over 20 FPS. Our code is available on <https://github.com/yjh0410/YOWOv2>.

**Index Terms**—Spatio-temporal action detection, one-stage detection, spatial encoder, temporal encoder

## I. INTRODUCTION

**S**PATIO-temporal action detection (STAD) aims to detect action instances in the current frame. It has been widely applied, such as video surveillance [1] and somatosensory game [2].

Since the occurrence of action is a continuous concept on the level of time, some researchers [3]–[6] take advantage of the 3D CNN [7], [8] to extract spatio-temporal features from a video clip for accurate action detection. However, these 3D CNN-based frameworks suffer from the high computation as the heavy 3D CNN they deploy, causing too slow detection speed to run in real time.

Therefore, some other researchers [9]–[11] take advantage of the 2D CNN [12], [13] to build more efficient action detection frameworks. The central idea of these 2D CNN-based frameworks is to use a parameter-sharing 2D CNN to extract the spatial features frame by frame and put them into a buffer. After that, they only need to process the new input frame and put its spatial feature and the features in the buffer together to form the spatio-temporal features for the final detection. However, such a pipeline cannot sufficiently

model temporal association, and real-time detection can only be guaranteed under the input conditions of RGB streams. Once the optical flow is used, despite the performance gain, the speed is drastically reduced.

On the contrary, Köpüklü et al. [14] combine a 2D backbone [15] for spatial localization and a 3D backbone for spatio-temporal modeling to build a new single-stage action detector, You Only Watch Once (YOWO). To save YOWO from the high computation of 3D CNN, they design a series of efficient 3D CNNs [16] as the 3D backbone for efficient inference. After the backbones, YOWO deploys a channel encoder to fuse these two features for the final detection. With their designs, YOWO achieves excellent performance on the popular benchmarks. It is the fast action detector as it claims. However, YOWO still suffers from two disadvantages:

- YOWO is a one-level detector and performs the final detection on a low-level feature map, impairing the detection performance for small action instances.
- YOWO is an anchor-based method and has lots of anchor boxes with many hyperparameters, such as the number, size, and aspect ratio of anchor boxes. Those hyperparameters must be carefully artificially designed, impairing the generalization.

In summary, **designing a real-time detection framework for the spatio-temporal action detection task is still a challenge**.

In this paper, we propose a novel real-time action detector, YOWOv2. YOWOv2 consists of a 3D backbone and a multi-level 2D backbone. Thanks to our multi-level 2D backbone with a feature pyramid network (FPN) [17], a multi-level detection pipeline is designed for YOWOv2 to detect action instances of different scales. For the 3D backbone, we also adopt the efficient 3D CNNs [16] to save deployment time. Additionally, we take advantage of the anchor-free mechanism, avoiding the drawbacks of the anchor box. Since the anchor box is removed, we deploy a dynamic label assignment strategy, further improving the versatility of the YOWOv2. Moreover, we build various models of YOWOv2 including **YOWOv2-Tiny**, **YOWOv2-Medium** and **YOWOv2-Large** by combining 3D backbones and 2D backbones of different sizes for the platforms with different computing power.

Compared with YOWO, YOWOv2 achieves better performance on the UCF101-24 [18] and AVA [19] datasets and also has significant advantages in both the number of parameters and the FLOPs. In addition, YOWOv2 still can run in real time. Compared with other real-time action detectors,

<sup>1</sup>Jianhua Yang and Kun Dai are with the State Key Laboratory of Robotics and System, Harbin Institute of Technology, Harbin 150001, China.

YOWOv2 also achieves better performance. Our contributions are summarized as follows:

- We propose a new real-time action detection framework, YOWOv2 with a multi-level detection structure, which is friendly to detect small action instances.
- YOWOv2 enjoys an anchor-free detection pipeline, avoiding the drawbacks of the anchor boxes.
- We design a YOWOv2 family by combining the 3D backbones and 2D backbones of different sizes for the platforms with different computing power.
- YOWOv2 achieves state-of-the-art performance on popular benchmarks, compared to other real-time action detectors.

## II. RELATED WORK

### A. Spatio-temporal action detection

Spatio-temporal action detection requires an action detector to locate and identify all action instances that occur in the current frame. How to effectively extract spatio-temporal features is essential for accurate action detection.

**3D CNN-based methods.** Some researchers use the 3D CNN to design action detectors [3], [4], [20]–[23], due to the strong spatio-temporal modeling capabilities. Girdhar et al. [3] use the I3D [7] to generate action region proposals and then use the Transformer [24] to complete the final detection. Zhao et al. [5] deploy a 3D CNN to encode input video and then use the Transformer with the tuber queries for final detection. Although these 3D CNN-based methods achieve impressive success, they all suffer from the expensive computation of the heavy 3D CNN and are therefore too slow to run in real time.

**2D CNN-based methods.** Another way is to decouple spatio-temporal associations and design 2D CNN-based action detectors for efficient detection. Kalogeiton et al. [9] design a one-stage detection framework, ActionTubelet (ACT). They first use the SSD [12] to extract spatial features from each frame of a video clip and then stack them together. Then, they use a detection head to process stacked spatial features for the final detection. Li et al. [11] follow the ACT framework and design an anchor-free one-stage action detector, MovingCenter (MOC). Ma et al. [25] enhance the MOC with the self-attention mechanism. However, the real-time detection of those methods can only be guaranteed under the input conditions of RGB streams. Once the optical flow is added, despite the performance gain, their speed is drastically reduced. Moreover, the high-quality optical flow needs to be obtained offline, which cannot satisfy online operations.

## III. METHODOLOGY

### A. Preliminary

The overview of YOWOv2 is shown in Fig.1. Given a video clip with  $K$  frames  $V = \{I_1, I_2, \dots, I_K\}$  where the  $I_K$  is the current frame, YOWOv2 uses an efficient 3D CNN [16] as the 3D backbone to extract spatio-temporal features  $F_{ST} \in \mathbb{R}^{\frac{H}{32} \times \frac{W}{32} \times C_{o2}}$ . The 2D backbone of YOWOv2 is a multi-level 2D CNN, responsible for outputting decoupled multi-level spatial features  $F_{cls} = \{F_{cls_i}\}_{i=1}^3$  and  $F_{reg} =$

$\{F_{reg_i}\}_{i=1}^3$  of  $I_K$ , where the  $F_{cls_i} \in \mathbb{R}^{\frac{H}{2^{i+2}} \times \frac{W}{2^{i+2}} \times C_{o1}}$  is the classification features and  $F_{reg_i} \in \mathbb{R}^{\frac{H}{2^{i+2}} \times \frac{W}{2^{i+2}} \times C_{o1}}$  is the regression features. After the two backbones, we deploy two channel encoders on each feature map of level to integrate features. After that, two extra parallel branches with two  $3 \times 3$  conv layers followed the channel encoders to predict  $Y_{cls_i} \in \mathbb{R}^{\frac{H}{2^{i+2}} \times \frac{W}{2^{i+2}} \times N_C}$  for classification,  $Y_{reg_i} \in \mathbb{R}^{\frac{H}{2^{i+2}} \times \frac{W}{2^{i+2}} \times 4}$  for regression respectively. A confidence branch is added on the regression branch to predict  $Y_{conf_i} \in \mathbb{R}^{\frac{H}{2^{i+2}} \times \frac{W}{2^{i+2}} \times 1}$  for actionness confidence. Next, we introduce the design of YOWOv2 in detail.

### B. Design of YOWOv2

**2D backbone.** The 2D backbone is supposed to extract multi-level spatial features from the current frame. Considering the balance between performance and speed, we draw some advanced ideas from the advanced object detectors [26], [27]. We reuse the backbone and feature pyramid network (FPN) of YOLOv7 [26] to save training time. After the FPN, we add extra  $1 \times 1$  conv layers to compress the channel number of each level feature map  $F_{S_i}$  to  $C_{o1}$  which is defaulted to 256. Then, we add two parallel branches with two  $3 \times 3$  conv layers to output decoupled features, as shown in Eq.(1).

$$\begin{aligned} F_{cls_i} &= f_{conv2}^1 (f_{conv1}^1 (F_{S_i})) \\ F_{reg_i} &= f_{conv2}^2 (f_{conv1}^2 (F_{S_i})) \end{aligned} \quad (1)$$

where the  $f_{conv_j}^i$  is the  $j^{th}$   $3 \times 3$  conv layer of the  $i^{th}$  branch.

In YOWOv2 framework, the 2D backbone outputs the decoupled feature maps of three levels,  $F_{cls} = \{F_{cls_i}\}_{i=1}^3$  and  $F_{reg} = \{F_{reg_i}\}_{i=1}^3$ . We name the 2D backbone FreeYOLO for convenience. By controlling the depth and width of FreeYOLO, we designed two FreeYOLO of different sizes, FreeYOLO-Tiny for YOWOv2-Tiny and FreeYOLO-Large for YOWOv2-Medium and YOWOv2-Large. To accelerate the convergence of training, we pretrain our 2D backbone with additional  $1 \times 1$  conv layers on the COCO [28]. The pretrained weight files are available on the GitHub<sup>1</sup>.

**3D backbone.** The 3D backbone is supposed to extract the spatio-temporal features  $F_{ST}$  from the video clip for the spatio-temporal association. We deploy the efficient 3D CNN [16] to reduce computation and thus guarantee real-time detection. To fuse with decoupled spatial features, we simply upsample  $F_{ST}$  to obtain  $\{F_{ST_i}\}_{i=1}^3$ , as shown in Eq.(2).

$$\begin{aligned} F_{ST_1} &= \text{Upsample}_{4 \times} (F_{ST}) \\ F_{ST_2} &= \text{Upsample}_{2 \times} (F_{ST}) \\ F_{ST_3} &= F_{ST} \end{aligned} \quad (2)$$

where the **Upsample** is the upsampling operation for aligning  $F_{ST_i} \in \mathbb{R}^{\frac{H}{2^{i+2}} \times \frac{W}{2^{i+2}} \times C_{o2}}$  and  $F_{cls_i}$  and  $F_{reg_i}$  in the spatial dimension.

**ChannelEncoder.** ChannelEncoder, proposed by YOWO [14], is supposed to fuse the features from the 2D backbone and 3D backbone. Given a  $F_S \in \mathbb{R}^{H_o \times W_o \times C_{o1}}$  and a  $F_{ST} \in \mathbb{R}^{H_o \times W_o \times C_{o2}}$ , the ChannelEncoder first concatenates

<sup>1</sup><https://github.com/yjh0410/FreeYOLO>

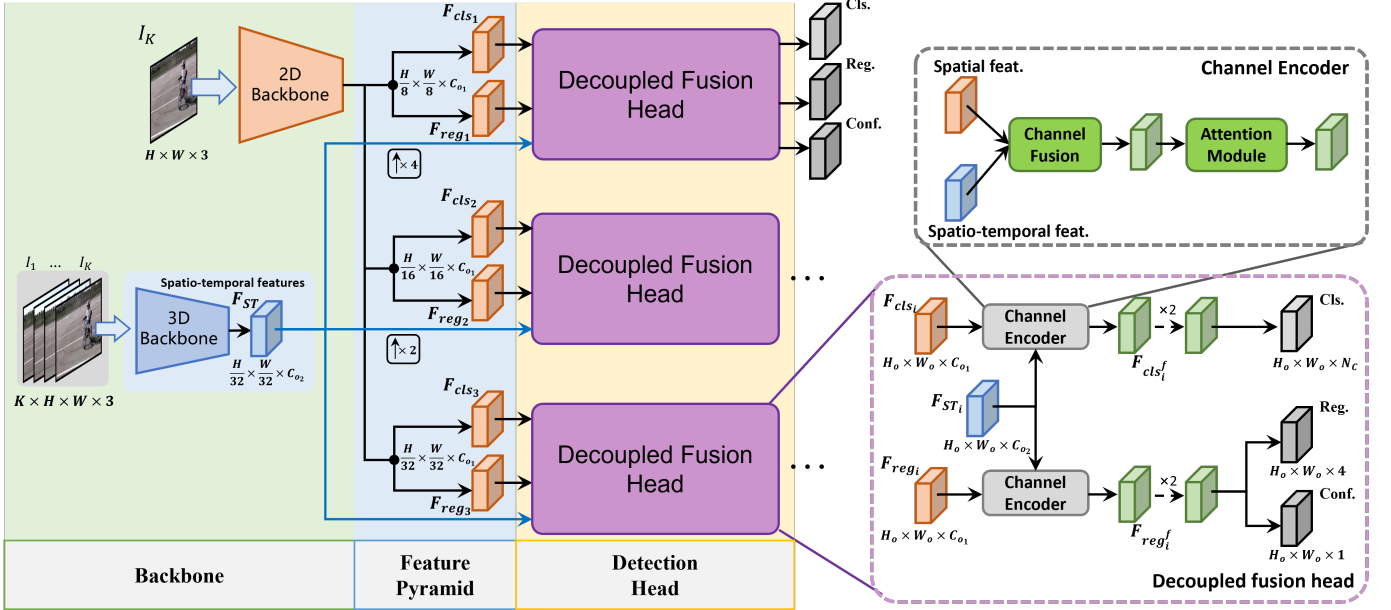


Fig. 1. Overview of YOWOv2. YOWOv2 uses upsampling operation to align the spatio-temporal features output by the 3D backbone with the spatial features of each level output by the 2D backbone and uses the Decoupled fusion head to achieve the fusion of the two features on each level. Finally, YOWOv2 outputs the multi-level confidence predictions, classification predictions, and regression predictions respectively.

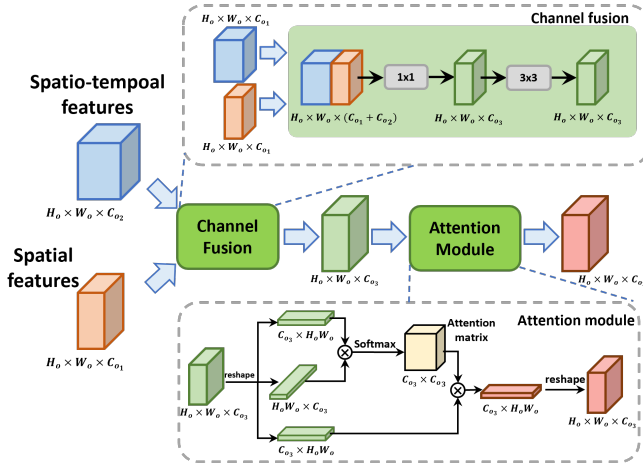


Fig. 2. Overview of ChannelEncoder. It contains the channel fusion and channel self-attention mechanism, which are both used to fuse 2D and 3D features.

them along the channel dimension and uses two naive conv layer followed a BN and LeakyReLU to achieve primary channel integration, as following,

$$F_f = f_{conv2} (f_{conv1} (\text{Concat} [F_S, F_{ST}])) \quad (3)$$

where the  $F_f \in \mathbb{R}^{H_o \times W_o \times C_{o3}}$ ,  $\text{Concat}$  is the channel concatenation operation,  $f_{conv1}$  and  $f_{conv2}$  are both the conv layers with BN and LeakyReLU. Then, the  $F_f$  is reshaped to  $F_{f2} \in \mathbb{R}^{C_{o3} \times H_o W_o}$  for the following channel self-attention mechanism inspired by DANet [29] to do deeper processing, so that the information containing two different levels features can be fully integrated, as shown in Eq.(4)

$$F_{f3} = \text{Softmax} (F_{f2} F_{f2}^T) F_{f2} \quad (4)$$

Finally, the  $F_{f3} \in \mathbb{R}^{C_{o3} \times H_o W_o}$  is reshaped to  $F_f \in \mathbb{R}^{H_o \times W_o \times C_{o3}}$  followed by another conv layer. The whole pipeline of the ChannelEncoder is shown in Fig.2.

**Decoupled fusion head.** In YOWOv2, the 2D backbone outputs the decoupled spatial features  $F_{cls} = \{F_{cls_i}\}_{i=1}^3$  and  $F_{reg} = \{F_{reg_i}\}_{i=1}^3$  of the current frame  $I_K$  while the 3D backbone outputs  $\{F_{ST_i}\}_{i=1}^3$  obtained by upsampling  $F_{ST}$  of the video clip  $V = \{I_1, I_2, \dots, I_K\}$ . Note that  $F_{cls_i}$  and  $F_{reg_i}$  contain very different semantic information, which inspires us to fuse  $F_{cls_i}$  and  $F_{reg_i}$  with  $F_{ST_i}$  separately. Therefore, we design a decoupled fusion head to fuse  $F_{ST_i}$  into  $F_{cls_i}$  and  $F_{reg_i}$  independently, as shown in Eq.(5).

$$\begin{aligned} F_{cls_i}^f &= \text{ChannelEncoder} (F_{cls_i}, F_{ST_i}) \\ F_{reg_i}^f &= \text{ChannelEncoder} (F_{reg_i}, F_{ST_i}) \end{aligned} \quad (5)$$

After the feature aggregation, we deploy two parallel branches on each level for final detection. Its design is simple, just a classification branch and a box regression branch.

For the classification branch, it outputs the classification prediction  $Y_{cls_i} \in \mathbb{R}^{\frac{H}{2^{i+2}} \times \frac{W}{2^{i+2}} \times N_C}$ , where  $Y_{cls_i}(x, y)$  represents the probability of action instances at each spatial position on  $Y_{cls_i}$  and  $N_C$  is the number of action classes. Taking  $F_{cls_i}^f$ , the branch applies two  $3 \times 3$  conv layers, each with  $C$  filters and each followed by SiLU activations. Finally, a  $1 \times 1$  conv layer with  $N_C$  filters and sigmoid activations is attached to output the  $N_C$  binary predictions per spatial position.

For the box regression branch, it outputs the box regression prediction  $Y_{reg_i} \in \mathbb{R}^{\frac{H}{2^{i+2}} \times \frac{W}{2^{i+2}} \times 4}$ , where  $Y_{reg_i}(x, y)$  represents the 4 relative offsets at each spatial position. The design is equal to the classification branch except that the final  $1 \times 1$  conv layer is with 4 filters for offset predictions. Additionally, an extra  $1 \times 1$  conv layer with 1 filter is added into this branch

for actionness confidence prediction,  $Y_{conf_i} \in \mathbb{R}^{\frac{H}{2^{i+2}} \times \frac{W}{2^{i+2}} \times 1}$ . Note that, there is no anchor box in each spatial position, therefore, YOWOv2 is an anchor-free method.

### C. Label assignment

Since the YOWOv2 is an anchor-free action detector without any anchor boxes, the first to bear the brunt is the multi-level label assignment. Recently, the dynamic label assignment has been successful in object detection. Inspired by YOLOX [27], we deploy the SimOTA for the label assignment of YOWOv2. Specifically, we calculate the cost between all predicted bounding boxes and groundtruths. The Eq.(6) shows the cost between  $i^{th}$  prediction and  $j^{th}$  groundtruth. Then each groundtruth is assigned with the  $top_k$  predicted bounding boxes with the least cost, where the  $k$  is dynamically determined by the IoU between the predicted bounding boxes and the target bounding boxes.

$$c_{ij} (\hat{a}_i, a_j, \hat{b}_i, b_j) = L_{cls}(\hat{a}_i, a_j) + \gamma L_{seg}(\hat{b}_i, b_j) \quad (6)$$

where the  $\hat{a}_i$  and  $a_j$  are the classification prediction (multiplied by confidence prediction) and target,  $\hat{b}_i$  and  $b_j$  are the regression prediction and target and  $\gamma$  is the cost balance factor, empirically being 3 in the experiments.

### D. Loss function

We define loss function as follows:

$$\begin{aligned} L(\{a_{x,y}\}, \{b_{x,y}\}, \{c_{x,y}\}) = & \frac{1}{N_{pos}} \sum_{x,y} L_{conf}(\hat{c}_{x,y}, c_{x,y}) \\ & + \frac{1}{N_{pos}} \sum_{x,y} \mathbb{I}_{\{\hat{a}_{x,y} > 0\}} L_{cls}(\hat{a}_{x,y}, a_{x,y}) \\ & + \frac{\lambda}{N_{pos}} \sum_{x,y} \mathbb{I}_{\{\hat{a}_{x,y} > 0\}} L_{reg}(\hat{b}_{x,y}, b_{x,y}) \end{aligned} \quad (7)$$

where  $L_{cls}$  is the binary cross-entropy and  $L_{reg}$  is the GIoU loss [30]. The  $a_{x,y}$ ,  $b_{x,y}$  and  $c_{x,y}$  are classification prediction, regression prediction, and confidence prediction, while the  $\hat{a}_{x,y}$ ,  $\hat{b}_{x,y}$  and  $\hat{c}_{x,y}$  are groundtruths.  $N_{pos}$  denotes the number of positive samples and  $\lambda$  is the loss balance factor, empirically being 5 in the experiments.  $I_{\{\hat{a}_{x,y} > 0\}}$  is the indicator function, being 1 if  $\hat{a}_{x,y} > 0$  and 0 otherwise.

## IV. EXPERIMENTS

### A. Datasets

**UCF101-24** [18]. UCF101-24 contains 3,207 untrimmed videos for 24 sports classes and provides corresponding spatio-temporal annotations. There may be multiple action instances per frame. Following YOWO [14], we train and evaluate YOWO-Plus on the first split.

**AVA** [19]. AVA is a large-scale benchmark for spatial-temporal action detection. It contains 430 15-minute video clips with 80 atomic visual actions (AVA). It provides annotations at 1 Hz in space and time, and precise spatio-temporal annotations with possibly multiple annotations for

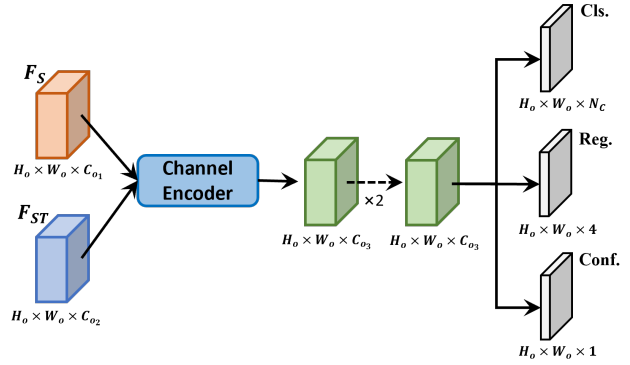


Fig. 3. Coupled fusion head. In the coupled head, the spatial features from the 2D backbone is also coupled which means that the parallel  $3 \times 3$  conv layers after the FPN are removed.

TABLE I  
PERFORMANCE COMPARISON BETWEEN COUPLED FUSION HEAD (CFH)  
AND DECOUPLED FUSION HEAD (DFH) ON THE UCF101-24.

Head	Model	FPS	F-mAP (%)	V-mAP (%)
CFH	YOWOv2-T	56	78.9	49.8
	YOWOv2-M	45	81.2	50.7
	YOWOv2-L	33	84.3	51.5
DFH	YOWOv2-T	50	80.5	51.3
	YOWOv2-M	42	83.1	50.7
	YOWOv2-L	30	<b>85.2</b>	<b>52.0</b>

each person. Therefore, this benchmark is very challenging. We train YOWOv2 on the train split and evaluate it on the most-frequent 60 action classes of the AVA dataset. We report evaluation results on the AVA v2.2.

### B. Implementation details

For training, we use the AdamW optimizer with an initial learning rate 0.0001 and weight decay 0.0005. The batch size is set to 8 with 16 gradient accumulate. On the UCF101-24, we train YOWOv2 for 7 epochs and decay the learning rate by a factor of 2 at 1, 2, 3, and 4 epoch, respectively. On the AVA, we train YOWOv2 for 9 epochs and decay the learning rate by a factor of 2 at 3, 4, 5, and 6 epoch, respectively. Unless otherwise specified, the size of the input frame is reshaped to  $224 \times 224$ .

For evaluation metrics, we follow previous works [5], [14], [22] to report frame mAP (F-mAP) and video mAP (V-mAP) at 0.5 IoU between predictions and groundtruths. We follow the link algorithm of YOWO [14] to build action tubelets. On the AVA, we report frame mAP at 0.5 IoU since the annotations are sparsely provided at 1 Hz.

### C. Effectiveness of decoupled fusion head

We first verify the effect of decoupled fusion head on YOWOv2. To achieve this goal, we also design a coupled fusion head as a control group, as shown in Fig.3. Table.I summarizes the comparison results on the UCF101-24. From the table, we find that the decoupled fusion head achieves

TABLE II

COMPARISON WITH YOWO ON THE UCF101-24. FPS IS MEASURED ON A GPU RTX 3090. K IS THE LENGTH OF THE VIDEO CLIP.

Method	K	FPS	F-mAP (%)	V-mAP (%)	GFLOPs	Params
YOWO	16	34	80.4	48.8	43.7	121.4 M
YOWO+LFB	-	-	87.3	53.1	-	-
YOWOv2-T	16	50	80.5	51.3	2.9	10.9 M
YOWOv2-M	16	42	83.1	50.7	12.0	52.0 M
YOWOv2-L	16	30	85.2	52.0	53.6	109.7 M
YOWOv2-T	32	50	83.0	51.2	4.5	10.9 M
YOWOv2-M	32	40	83.7	52.5	12.7	52.0 M
YOWOv2-L	32	22	87.0	52.8	91.9	109.7 M

TABLE III

COMPARISON WITH YOWO ON THE AVA. FPS IS MEASURED ON A GPU RTX 3090.

Method	K	FPS	mAP
YOWO	16	31	17.9
YOWO	32	23	19.1
YOWO+LFB	-	-	20.2
YOWOv2-T	16	49	14.9
YOWOv2-M	16	41	18.4
YOWOv2-L	16	29	20.2
YOWOv2-T	32	49	15.6
YOWOv2-M	32	40	18.4
YOWOv2-L	32	22	21.7

better performance. The experimental results demonstrate that feature fusion should be performed decoupled due to the semantic differences between categorical and regressive features. Although the decoupled fusion head hurts the detection speed slightly, the significant performance gain makes up for the marginal loss in speed.

#### D. Comparison with YOWO

Next, we compare the accuracy, speed, and computation with YOWO [14]. By combining different 3D backbones and 2D backbones, we designed a total of three scales of YOWOv2, YOWOv2-Tiny (YOWOv2-T), YOWOv2-Medium (YOWOv2-M) and YOWOv2-Large (YOWOv2-L). To demonstrate the superiority and balance of YOWOv2 in terms of speed and performance, we compare our YOWOv2 family with YOWO on the UCF101-24 benchmark. Table.II summarizes the comparison results. From the table, the YOWOv2-T achieves better performance on both metrics frame mAP (80.5 % v.s. 80.4 %) and video mAP (51.3 % v.s. 48.8 %) with much fewer FLOPs (2.9 G v.s. 43.7 G), parameters (10.9 M v.s. 121.4 M) and higher FPS (50 v.s. 34) on an RTX 3090 GPU. Equipped with a stronger 2D backbone and 3D backbone, YOWOv2-L achieves the best performance. Fig.4 shows the per-class AP comparison results between YOWO and YOWOv2-L.

Only equipped with a long-term feature bank (LFB) [31], YOWO can competitive performance with YOWOv2. However, LFB module makes the YOWO an acausal detector since it uses the future information for inference, so it can only run offline.

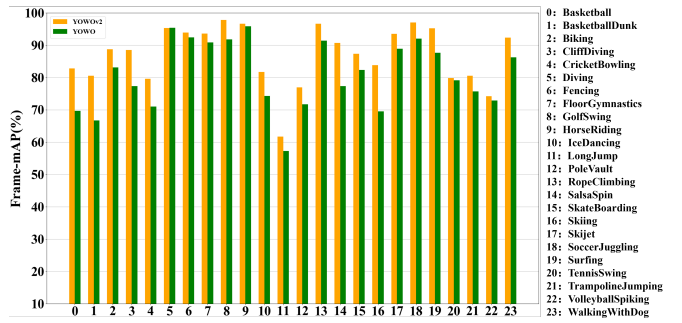


Fig. 4. Per-class frame mAP at 0.5 IoU on the UCF101-24. The orange bars represent the per-class AP of YOWOv2-L, while the green bars represent the per-class AP of YOWO.

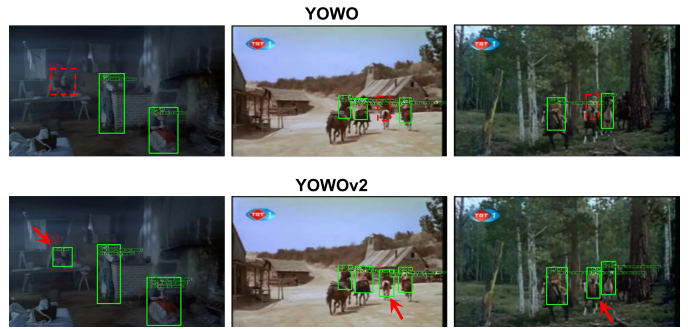


Fig. 5. Performance comparison of small action instance detection between YOWO and YOWOv2 on the AVA.

Besides UCF101-24, we also do a comparative experiment with YOWO on the AVA benchmark. Table.III summarizes the comparison results. Since the AVA is a very challenging dataset, it is unrealistic to expect the tiny YOWOv2-T to surpass YOWO which has larger calculations and more parameters. Here, we mainly pay attention to the YOWOv2-L. Compared to YOWO, YOWOv2-L achieves a better trade-off between performance and detection speed. YOWOv2 also outperforms the YOWO with the LFB. The advantages on these popular benchmarks prove that the design of YOWOv2 is superior to the previous generation of YOWO, achieving the purpose of inheritance and development, and realizing a new generation of real-time motion detection framework.

On the other hand, we compare the performance of small action instance detection on the AVA with YOWO to demonstrate the effectiveness of the multi-level detection of YOWOv2, as shown in Fig.5. From the figure, we can find that YOWO is not confident enough about some smaller action instances, leading to missed detection (red dotted line boxes). Equipped with the multi-level detection pipeline, YOWOv2 can better detect the smaller action instances that YOWO cannot cope with.

#### E. Comparison with other real-time action detectors

Besides YOWO, we also compare YOWOv2 with other real-time action detectors. Fig.6 shows the speed/accuracy trade-off of those detectors that can run at over 25 FPS on an RTX 3090 GPU, including YOWO [14], MOC [11], SAMOC [25] and ACT [9]. From the figure, YOWOv2 achieves a significantly better trade-off between performance and detection speed.

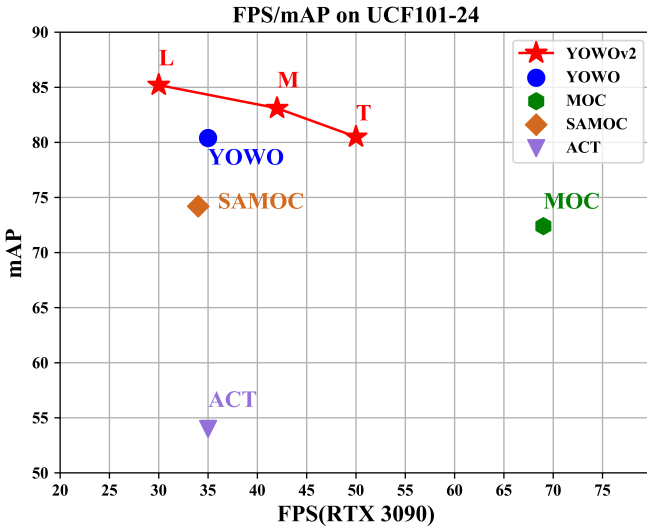


Fig. 6. Speed/accuracy trade-off among multiple real-time action detectors, including YOWO, MOC, SAMOC, ACT and the proposed YOWOv2. Speed is measured on an NVIDIA 3090 GPU with batch size 1. Note that the length of the input video clip is 16 YOWO and YOWOv2.

TABLE IV

COMPARISON WITH STATE-OF-THE-ART WORKS ON THE UCF101-24. WE REPORT FRAME MAP AT 0.5 IOU AND VIDEO MAP AT 0.5 IOU ON THE FIRST SPLIT.

Method		RGB	Flow	F-mAP (%)	V-mAP (%)
3D	T-CNN [20]	✓	✗	41.4	-
	I3D [19]	✓	✓	76.6	<b>59.9</b>
	Tuber [5]	✓	✗	83.2	58.4
2D	ACT [9]	✓	✓	67.1	51.4
	TACNet [10]	✓	✓	72.1	54.4
	MOC [11]	✓	✗	73.1	51.0
	MOC [11]	✓	✓	78.0	53.8
	SAMOC [25]	✓	✗	74.2	49.8
	SAMOC [25]	✓	✓	79.3	52.5
	YOWOv2-T	✓	✗	80.5	51.3
	YOWOv2-M	✓	✗	83.1	50.7
	YOWOv2-L	✓	✗	85.2	52.0
	YOWOv2-T (K=32)	✓	✗	83.0	51.2
	YOWOv2-M (K=32)	✓	✗	83.7	52.5
	YOWOv2-L (K=32)	✓	✗	<b>87.0</b>	52.8

Therefore, YOWOv2 may be regarded as a new generation of excellent real-time motion detectors.

#### F. Comparison with state-of-the-art works

**UCF101-24.** We train YOWOv2 with  $K = 16$  and sampling rate 4 ( $16 \times 4$ ). For stronger performance, we also use  $K = 32$  to train and test YOWOv2. Table.IV summarizes the comparison results with state-of-the-art works on the UCF101-24. From the table, most 2D CNN-based detectors use optical flow in parallel with the video clip to extract richer spatio-temporal features to enhance their performance. However, using optical flow not only limits the practicality of the model as the difficulty of obtaining high-quality optical flow online in real-time but also slows down the detection speed. Even compared with the powerful 3D CNN-based methods, our real-time YOWOv2 still shows competitive performance.

TABLE V  
COMPARISON WITH STATE-OF-THE-ART WORKS ON THE AVA. WE REPORT MAP AT 0.5 IOU ON THE AVA VALIDATION SPLIT.

Method	3D Backbone	Input	mAP (%)	GFLOPs
I3D [19]	I3D-VGG	$32 \times 2$	14.5	-
SlowFast [8]	SlowFast-R50	$16 \times 4$	24.2	308
X3D-XL [32]	X3D-XL	$16 \times 5$	26.1	290
WOO [22]	SlowFast-R101	$8 \times 4$	28.3	252
Tuber [5]	I3D-ResNet50	$16 \times 4$	26.1	132
Tuber [5]	I3D-ResNet101	$16 \times 4$	28.6	246
Tuber* [5]	CSN-152	$32 \times 2$	31.7	120
YOWO [14]	3D-ResNeXt-101	$16 \times 4$	17.9	44
YOWO [14]	3D-ResNeXt-101	$32 \times 4$	19.1	82
YOWOv2-T	3D-ShuffleNetv2-1.0x	$16 \times 4$	14.9	2.9
YOWOv2-M	3D-ShuffleNetv2-2.0x	$16 \times 4$	18.4	12.1
YOWOv2-L	3D-ResNeXt-101	$16 \times 4$	20.3	53.6
YOWOv2-T	3D-ShuffleNetv2-1.0x	$32 \times 4$	15.6	4.5
YOWOv2-M	3D-ShuffleNetv2-2.0x	$32 \times 4$	18.4	13.7
YOWOv2-L	3D-ResNeXt-101	$32 \times 4$	21.7	92.0

**AVA.** Table.V summarizes the comparison results on the AVA. Since the AVA is a very challenging benchmark where the data scene is changeable, and each action instance is labeled with multiple annotations, most current works are based on 3D CNN to challenge this dataset. We mainly compare with 3D CNN-based methods here, including YOWO [14]. From the table, 3D CNN-based methods show powerful spatio-temporal action detection performance, significantly stronger than YOWOv2. However, their GFLOPs are so high that they can hardly keep real-time detection. Tuber [5] is one of the latest state-of-the-art detectors, which consists of 3D CNN as the backbone and Transformer. It achieves 28.6 % mAP on the AVA, but its GLOPs are as high as 246, severely slowing down Tuber. Although Tuber\* achieves better performance (31.7 % mAP) with fewer GFLOPs (120), it is a two-stage model, which cannot be end-to-end trained or make an end-to-end inference. Compared to these 3D CNN-based works, YOWOv2 achieves competitive performance with relatively fewer FLOPs and can run in real time, though there is still a gap between YOWOv2 and other advanced detectors. Fig.7 shows some qualitative results on the AVA.

#### G. Test in real scenarios

To demonstrate the generalization of YOWOv2, we also test the performance of YOWOv2 in real scenarios. Fig.8 shows a demo of YOWOv2 in a real scene. The input frame is reshaped to  $224 \times 224$ , following the requirements in Sec.IV-B. Since most of the atomic actions in the AVA dataset do not appear in our real scenes, we only show fourteen basic action poses [19] in Fig.8, including bend or bow, crawl, stand, walk, sit, etc. From the figure, we can see that YOWOv2 still works well in real scenarios, demonstrating its effectiveness and generalization.

## V. CONCLUSION

In this paper, we propose a novel real-time detection framework YOWOv2 for spatial-temporal action detection. The YOWOv2 family contains YOWOv2-Tiny, YOWOv2-Medium, and YOWOv2-Large for the platforms with different computing power. Compared to the previous version



Fig. 7. Qualitative results on the AVA.

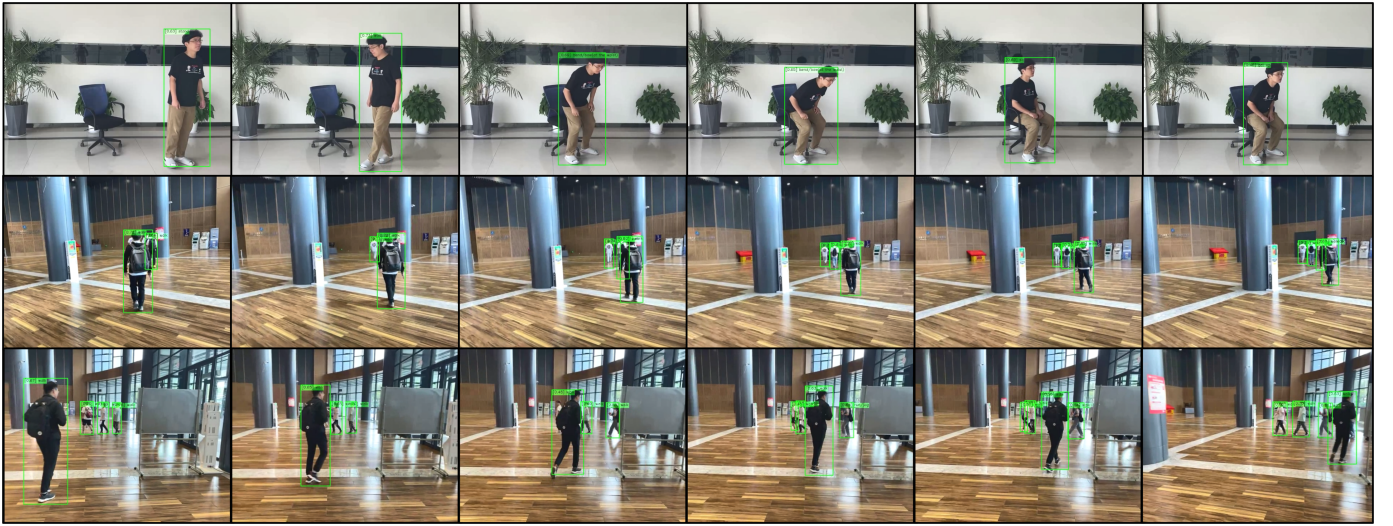


Fig. 8. Qualitative results on real scene. Since most of the atomic actions in the AVA dataset do not appear in our real scenes, we only show fourteen basic action poses, including bend or bow, crawl, stand, walk, sit, etc. The green bounding box represents the spatial localization. The action category with confidence score is shown in the upper left corner of the bounding box.

of YOWO, our YOWOv2 is designed as a multi-level action detection framework, helping to detect smaller motion instances. YOWOv2 is also an anchor-free action detector, avoiding the drawbacks of anchor boxes existing in YOWO. On the popular benchmarks, YOWOv2 significantly outperforms YOWO and other real-time action detectors with a large gap. Even compared with powerful but no speed advantage 3D CNN-based methods, YOWOv2 still shows competitive performance. YOWOv2 is an effective attempt, but it is not the end of YOWO. In the future, we will further study to design a more efficient and powerful feature pyramid network to fuse multi-level features from both the 3D backbone and 2D backbone, not just the 2D backbone.

## REFERENCES

- [1] A. Clapés, À. Pardo, O. Pujol Vila, and S. Escalera, “Action detection fusing multiple kinects and a wimu: An application to in-home assistive technology for the elderly,” *Machine Vision and Applications*, vol. 29, no. 5, pp. 765–788, 2018.
- [2] C. Yan, Y. Tu, X. Wang, Y. Zhang, X. Hao, Y. Zhang, and Q. Dai, “Stat: Spatial-temporal attention mechanism for video captioning,” *IEEE transactions on multimedia*, vol. 22, no. 1, pp. 229–241, 2019.
- [3] R. Girdhar, J. Carreira, C. Doersch, and A. Zisserman, “Video action transformer network,” in *Proceedings of the IEEE/CVF conference on computer vision and pattern recognition*, pp. 244–253, 2019.
- [4] J. Wu, Z. Kuang, L. Wang, W. Zhang, and G. Wu, “Context-aware rccn: A baseline for action detection in videos,” in *European Conference on Computer Vision*, pp. 440–456, Springer, 2020.
- [5] J. Zhao, Y. Zhang, X. Li, H. Chen, B. Shuai, M. Xu, C. Liu, K. Kundu, Y. Xiong, D. Modolo, *et al.*, “Tuber: Tubelet transformer for video action detection,” in *Proceedings of the IEEE/CVF Conference on Computer Vision and Pattern Recognition*, pp. 13598–13607, 2022.
- [6] S. Liu, M. Jiang, and J. Kong, “Multi-dimensional prototype refactor enhanced network for few-shot action recognition,” *IEEE Transactions on Circuits and Systems for Video Technology*, 2022.
- [7] J. Carreira and A. Zisserman, “Quo vadis, action recognition? a new model and the kinetics dataset,” in *proceedings of the IEEE Conference on Computer Vision and Pattern Recognition*, pp. 6299–6308, 2017.
- [8] C. Feichtenhofer, H. Fan, J. Malik, and K. He, “Slowfast networks for video recognition,” in *Proceedings of the IEEE/CVF international conference on computer vision*, pp. 6202–6211, 2019.
- [9] V. Kalogeiton, P. Weinzaepfel, V. Ferrari, and C. Schmid, “Action tubelet detector for spatio-temporal action localization,” in *Proceedings of the*

*IEEE International Conference on Computer Vision*, pp. 4405–4413, 2017.

[10] L. Song, S. Zhang, G. Yu, and H. Sun, “Tacnet: Transition-aware context network for spatio-temporal action detection,” in *Proceedings of the IEEE/CVF Conference on Computer Vision and Pattern Recognition*, pp. 11987–11995, 2019.

[11] Y. Li, Z. Wang, L. Wang, and G. Wu, “Actions as moving points,” in *European Conference on Computer Vision*, pp. 68–84, Springer, 2020.

[12] W. Liu, D. Anguelov, D. Erhan, C. Szegedy, S. Reed, C.-Y. Fu, and A. C. Berg, “Ssd: Single shot multibox detector,” in *European conference on computer vision*, pp. 21–37, Springer, 2016.

[13] X. Zhou, D. Wang, and P. Krähenbühl, “Objects as points,” *arXiv preprint arXiv:1904.07850*, 2019.

[14] O. Köpüklü, X. Wei, and G. Rigoll, “You only watch once: A unified cnn architecture for real-time spatiotemporal action localization,” *arXiv preprint arXiv:1911.06644*, 2019.

[15] J. Redmon and A. Farhadi, “Yolo9000: better, faster, stronger,” in *Proceedings of the IEEE conference on computer vision and pattern recognition*, pp. 7263–7271, 2017.

[16] O. Kopuklu, N. Kose, A. Gunduz, and G. Rigoll, “Resource efficient 3d convolutional neural networks,” in *Proceedings of the IEEE/CVF International Conference on Computer Vision Workshops*, pp. 0–0, 2019.

[17] T.-Y. Lin, P. Dollár, R. Girshick, K. He, B. Hariharan, and S. Belongie, “Feature pyramid networks for object detection,” in *Proceedings of the IEEE conference on computer vision and pattern recognition*, pp. 2117–2125, 2017.

[18] K. Soomro, A. R. Zamir, and M. Shah, “Ucf101: A dataset of 101 human actions classes from videos in the wild,” *arXiv preprint arXiv:1212.0402*, 2012.

[19] C. Gu, C. Sun, D. A. Ross, C. Vondrick, C. Pantofaru, Y. Li, S. Vijayanarasimhan, G. Toderici, S. Ricco, R. Sukthankar, *et al.*, “Ava: A video dataset of spatio-temporally localized atomic visual actions,” in *Proceedings of the IEEE Conference on Computer Vision and Pattern Recognition*, pp. 6047–6056, 2018.

[20] R. Hou, C. Chen, and M. Shah, “Tube convolutional neural network (t-cnn) for action detection in videos,” in *Proceedings of the IEEE international conference on computer vision*, pp. 5822–5831, 2017.

[21] K. Duarte, Y. Rawat, and M. Shah, “Videocapsulenet: A simplified network for action detection,” *Advances in neural information processing systems*, vol. 31, 2018.

[22] S. Chen, P. Sun, E. Xie, C. Ge, J. Wu, L. Ma, J. Shen, and P. Luo, “Watch only once: An end-to-end video action detection framework,” in *Proceedings of the IEEE/CVF International Conference on Computer Vision*, pp. 8178–8187, 2021.

[23] J. Pan, S. Chen, M. Z. Shou, Y. Liu, J. Shao, and H. Li, “Actor-context-actor relation network for spatio-temporal action localization,” in *Proceedings of the IEEE/CVF Conference on Computer Vision and Pattern Recognition*, pp. 464–474, 2021.

[24] A. Vaswani, N. Shazeer, N. Parmar, J. Uszkoreit, L. Jones, A. N. Gomez, Ł. Kaiser, and I. Polosukhin, “Attention is all you need,” *Advances in neural information processing systems*, vol. 30, 2017.

[25] X. Ma, Z. Luo, X. Zhang, Q. Liao, X. Shen, and M. Wang, “Spatiotemporal action detector with self-attention,” in *2021 International Joint Conference on Neural Networks (IJCNN)*, pp. 1–8, IEEE, 2021.

[26] C.-Y. Wang, A. Bochkovskiy, and H.-Y. M. Liao, “Yolov7: Trainable bag-of-freebies sets new state-of-the-art for real-time object detectors,” *arXiv preprint arXiv:2207.02696*, 2022.

[27] Z. Ge, S. Liu, F. Wang, Z. Li, and J. Sun, “Yolox: Exceeding yolo series in 2021,” *arXiv preprint arXiv:2107.08430*, 2021.

[28] T.-Y. Lin, M. Maire, S. Belongie, J. Hays, P. Perona, D. Ramanan, P. Dollár, and C. L. Zitnick, “Microsoft coco: Common objects in context,” in *European conference on computer vision*, pp. 740–755, Springer, 2014.

[29] J. Fu, J. Liu, H. Tian, Y. Li, Y. Bao, Z. Fang, and H. Lu, “Dual attention network for scene segmentation,” in *Proceedings of the IEEE/CVF conference on computer vision and pattern recognition*, pp. 3146–3154, 2019.

[30] H. Rezatofighi, N. Tsai, J. Gwak, A. Sadeghian, I. Reid, and S. Savarese, “Generalized intersection over union: A metric and a loss for bounding box regression,” in *Proceedings of the IEEE/CVF conference on computer vision and pattern recognition*, pp. 658–666, 2019.

[31] C.-Y. Wu, C. Feichtenhofer, H. Fan, K. He, P. Krahenbuhl, and R. Girshick, “Long-term feature banks for detailed video understanding,” in *Proceedings of the IEEE/CVF Conference on Computer Vision and Pattern Recognition*, pp. 284–293, 2019.

[32] C. Feichtenhofer, “X3d: Expanding architectures for efficient video recognition,” in *Proceedings of the IEEE/CVF Conference on Computer Vision and Pattern Recognition*, pp. 203–213, 2020.